ISSN 0389-4010
UDC 533. 6. 69. 058:

TECHNICAL REPORT OF NATIONAL AEROSPACE LABORATORY

TR-661T

A Study on Numerical Method for Evaluating Spanwise Integral in Subsonic Lifting-Surface Theory

Teruo ICHIKAWA

March 1981

NATIONAL AEROSPACE LABORATORY

CHŌFU, TOKYO, JAPAN

A Study on Numerical Method for Evaluating Spanwise Integral in Subsonic Lifting-Surface Theory*

By Teruo ICHIKAWA**

ABSTRACT

Two disputable points in the spanwise integral in the NLR method are discussed. The first point is the coincidence of each collocation section with one of the spanwise integration points. This makes necessary the evaluation of the regularized influence functions at the coincident points, which is very time consuming except in cases of steady wings. The second point is the relatively small, but undesirable, sharp variation of the regularized influence functions near the collocation sections, which is the cause of the necessity of taking a large number of spanwise integration points. Two proposals for coping with these difficulties are made. We call these proposals Method 1 and Method 2. Their effects are examined by computing the downwash at the surface of a steady rectangular wing subjected to a simple wing loading. It is shown that Method 1, which avoids the coincidence, makes it possible, with no losses in accuracy, to greatly reduce the computing time in cases of oscillating wings. Further, it is shown that remarkable improvement in convergence with repect to the number of spanwise integration points is obtained by Method 2 which distributes the spanwise integration points densely only near the collocation sections.

概　　要

NLR の方法の翼幅方向積分における二つの問題点について考察した．第１の問題点は各標点断面が翼幅方向積分点の一つと一致することである．このため，この一致した点での正則化した影響関数の値を計算する必要があり，定常翼の場合を除いてこれは多大の計算時間を消費する．第２の問題点は正則化した影響関数が標点断面の近くで比較的小さいが望ましくない急激な変化をすることで，この事が翼幅方向積分点を多く取らなければならない原因となっている．これらの困難を解決する改善策として方法１と方法２を提案し，その効果を調べるため，簡単な形の空力荷重分布を持つ定常短形翼の翼面上の吹下ろしを計算した．方法１は上記の一致を避ける方法で，これによって振動翼の場合に精度を損なわずに計算時間を大幅に減らし得ることがわかった．また方法２は翼幅方向積分点を標点断面の付近でだけ密にする方法で，これによって吹下ろしの翼幅方向積分点数に関する収束性が著しく改善されることがわかった．

NOMENCLATURE

a	positive integer controlling number of spanwise integration points
$a_{r\lambda}$	coefficient, Eq. (33)
$\bar{a}_{r\lambda}$	coefficient, Eq. (39)
$a_{r\lambda}^{\nu}$	coefficient, Eq. (46)
A	aspect ratio
$A_{qr}(p, \nu)$	coefficient, Eq. (25)
$b_{\nu r}$	coefficient, Eq. (31)
$b(\eta_\nu)$	coefficient for rectangular wing, Eqs. (62) and (67)
$B_{qr}(p, \nu)$	coefficient, Eqs (30), (32), (38), and (45)
$B(\xi, \eta_\nu)$	coefficient for rectangular wing, Eqs. (61), (69), (70), and (71)
c	chord of rectangular wing

* Received February 13, 1981
** First Airframe Division

$c(y')$	local chord
$c_{\nu r}$	coefficient, Eq. (31)
$C_q(x, \eta)$	coefficient of logarithmic singularity in influence function
$C(\xi)$	coefficient of logarithmic singularity in influenice function for rectangular wing
$d_{\nu r}$	coefficient, Eq. (31)
$d(\eta_\nu)$	coefficient for rectangular wing, Eqs. (63) and (68)
$f(x)$	continuous function
$f_r^R(\theta)$	Multhopp's interpolation coefficient, Eq. (2)
$F_q(x, \eta; \eta')$	influence function, Eq. (24)
$F(\xi, \eta_\nu - \eta')$	influence function for rectangular wing, Eq. (54)
$F_\nu(\varphi)$	transforming function
$F_\nu^{(1)}(\varphi)$	transforming function of the first kind, Eqs. (72) and (73)
$F_\nu^{(2)}(\varphi)$	transforming function of the second kind, Eqs. (74) and (75)
$g_r^R(\theta)$	interpolation coefficient, Eqs. (6) and (8)
h	zero or positive integer controlling δ in Eq. (48)
$K(x, y; x', y')$	kernel function
$l(x', y')$	wing loading (lift per unit area) as a fraction of dynamic pressure
$l_r^R(x)$	Lagrangian interpolation coefficient, Eq. (A3)
m	number of collocation sections
M	Mach number of stream
N	number of chordwise loading functions or collocation points
p	integer denoting chordwise position of collocation point
$p_R(x)$	orthogonal polynomial of degree R satisfying Eq. (A4)
$P_q(x, \eta; \eta')$	modified influence function, Eq. (27)
$P(\xi, \eta_\nu - \eta')$	modified influence function for rectangular wing, Eq. (55)
q	integer denoting chordwise loading function
r	integer denoting Muthopp's abscissa for interpolating spanwise loading functions
$R_q(x, \eta; \eta')$	regularized influence function, Eq. (28)
$R(\xi, \eta_\nu - \eta')$	regularized influence function for rectangular wing, Eq. (58)
s	semispan of wing
$W(x)$	weight function
$x, y; x', y'$	rectangular coordinates in plane of wing
x_r	zero of polynomial $p_R(x)$
$x_l(y'), x_t(y')$	coordinates of leading and trailing edges, respectively
$x_{p\nu}$	coordinate of collocation point, Eq. (22)
$X, X_0; Y$	Eqs. (37)
y_ν	$=s\eta_\nu$
$\alpha(x, y)$	downwash angle (downwash as a fraction of stream velocity)
$\alpha_{p\nu}$	$=\alpha(x_{p\nu}, y_\nu)$
β	$=(1-M^2)^{1/2}$
$\Gamma_q(\eta')$	spanwise loading function
$\Gamma(\eta')$	spanwise loading function for rectangular wing
Γ_{qr}	$=\Gamma_q(\eta_r)$
δ	zero or positive real number controlling interval of φ in Fig. 2
η	$=y/s$
η'	$=y'/s$
η_r	$=-\cos\theta_r$
η_λ	$=-\cos\theta_\lambda$
$\bar{\eta}_\lambda$	$=-\cos\bar{\theta}_\lambda$
η_ν	$=-\cos\theta_\nu$
$\eta_{\nu\lambda}$	$=-\cos\theta_{\nu\lambda}$
θ'	$=\arccos(-\eta')$
θ_r	Multhopp's abscissa (angular coordinate) for interpolating spanwise loading functions, Eq. (19)
θ_λ	angular coordinate of spanwise integration point, Eq. (34)
$\bar{\theta}_\lambda$	angular coordinate of spanwise integration point, Eq. (40)
θ_ν	angular coordinate of control section, Eq. (20)
$\theta_{\nu\lambda}$	angular coordinate of spanwise integration point, Eq. (47)
λ	integer denoting panwise integration point
Λ	number of spanwise integration points, Eq. (34)
Λ_1	number of spanwise integration points, Eq. (41)
Λ_2	number of spanwise integration points, Eq. (48)
ν	integer denoting collocation section
ξ, ξ'	Eqs. (50)
ϕ	Eq. (51)
ϕ'	Eq. (17); for rectangular wing,

	Eq. (51)
ϕ_p	angular coordinate of chordwise position of collocation point, Eq. (22)
φ	angular variable in Fig. 2
φ_λ	Eq. (47)
Φ	Eq. (43)
Φ_λ	Eq. (47)
$\Psi_q(\phi')$	chordwise loading function
$\Psi(\phi')$	chordwise loading function for rectangular wing

1. INTRODUCTION

Among a variety of methods for solving the integral equation of the subsonic lifting-surface theory, Multhopp's method[1] and its improved versions seem to occupy important positions. P. T. Hsu[2] extended the Multhopp concept of optimum collocation points, and gave a new quadrature formula for the spanwise integral. Garner and Fox[3] used a larger number of spanwise integration points than that of collocation sections, and treated the logarithmic singularity of the influence function using the Mangler and Spencer method[4]. Zandbergen, Labrujere and Wouters[5] applied the Multhopp interpolation formula both to the spanwise loading function and to the regularized influence function separately, using their own mtehod for treating the logarithmic singularity. It is rather surprising that the concept of regularized influence function had been suggested earlier by Multhopp (Appendix V in Ref. 1). Of the above methods, Refs. 1 and 5 are for steady wings and Refs. 2 and 3 are for oscillating wings. Lehrian and Garner[6] extended the method of Ref. 5 (NLR method) to oscillating wings. Furthermore, Garner and his collaborators made a series of studies[7-9] to compare and appraise various methods.

This paper considers the spanwise integration in the NLR method, and proposes further improvements upon this. Although the numerical examples presented are confined to cases of the steady wing, the proposed methods should be applicable to those of the oscillating wing.

2. INTERPOLATION AND QUADRATURE FORMULAE

As a preliminary, two interpolation formulae and the related quadrature formulae are given. One of the interpolation formulae has been known.

Let a function $F(\theta)$ be defined in the interval $[0, \pi]$, and let $F(0)=F(\pi)=0$. Then the following interpolation formula has been given by Multhopp:[1,10]

$$F(\theta)\approx \sum_{r=1}^{R} F(\theta_r)f_r^R(\theta) \tag{1}$$

where

$$f_r^R(\theta)=\frac{(-1)^r \sin\theta_r \sin(R+1)\theta}{(R+1)(\cos\theta_r-\cos\theta)} = \frac{2}{R+1}\sum_{s=1}^{R}\sin s\theta_r \sin s\theta \tag{2}$$

$$\theta_r=\frac{r\pi}{R+1} \tag{3}$$

The interpolation coefficients $f_r^R(\theta)$ satisfy the conditions

$$\left.\begin{aligned} f_r^R(\theta_r)&=1 \\ f_r^R(\theta_p)&=0 \qquad p\neq r \end{aligned}\right\} \tag{4}$$

The abscissae θ_r are zeros of $\sin(R+1)\theta$ in the interval $[0, \pi]$.

Let us consider, next, interpolation coefficients $g_r^R(\theta)$ corresponding to abscissae

$$\bar{\theta}_r=\frac{(2r-1)\pi}{2R} \qquad r=1, 2, \cdots, R \tag{5}$$

which are zeros of $\cos R\theta$ in the interval $[0, \pi]$. By the same idea as that Multhopp adopted to derive $f_r^R(\theta)$, we have

$$g_r^R(\theta) = \frac{\cos R\theta}{(\cos\theta-\cos\theta_r)[d(\cos R\theta)/d(\cos\theta)]_{\theta=\bar{\theta}_r}} = \frac{(-1)^r \sin\bar{\theta}_r \cos R\theta}{R(\cos\bar{\theta}_r-\cos\theta)} \tag{6}$$

Eq. (6) has been constructed so as to satisfy the conditions

$$\left.\begin{aligned} g_r^R(\theta_r)&=1 \\ g_r^R(\theta_p)&=0 \qquad p\neq r \end{aligned}\right\} \tag{7}$$

By regarding the interpolation coefficients $g_r{}^R(\theta)$ as even functions in the interval $[-\pi, \pi]$, and through a similar procedure used by Multhopp to obtain the Fourier expansions of $f_r{}^R(\theta)$, we have the following finite cosine series as the Fourier expansions of $g_r{}^R(\theta)$:

$$g_r{}^R(\theta)=\frac{2}{R}\left(\frac{1}{2}+\sum_{s=1}^{R-1}\cos s\bar{\theta}_r \cos s\theta\right) \qquad (8)$$

It can be seen from Eqs. (7) and (8) that the coefficients $g_r{}^R(\theta)$ are suitable for interpolating a function $\bar{F}(\theta)$ which is defined in the interval $[0, \pi]$ and satisfies the condition $\bar{F}'(0)=\bar{F}'(\pi)=0$ where $\bar{F}'(\theta)$ means $d\bar{F}(\theta)/d\theta$, so that

$$\bar{F}(\theta)\approx\sum_{r=1}^{R}\bar{F}(\bar{\theta}_r)g_r{}^R(\theta) \qquad (9)$$

In the following, we shall need the quadrature formula for integrals of the type

$$I=\int_0^\pi G(\theta)d\theta \qquad (10)$$

with

$$G(\theta)=\bar{G}(\theta)\sin\theta \qquad (11)$$

where $\bar{G}(0)=\bar{G}(\pi)=0$ and therefore $G'(0)=G'(\pi)=0$. First, let us apply the interpolation formula, Eq. (1), to the function $\bar{G}(\theta)$. Then we have the first quadrature formula

$$I\approx\frac{1}{R+1}\sum_{r=1}^{R}(-1)^r\sin\theta_r\bar{G}(\theta_r)\times\int_0^\pi\frac{\sin(R+1)\theta\sin\theta}{\cos\theta_r-\cos\theta}d\theta=\frac{\pi}{R+1}\sum_{r=1}^{R}G(\theta_r) \qquad (12)$$

We can see that Eq. (12) is nothing but the simple trapezoidal rule since $G(0)=G(\pi)=0$.

Secondly, the application of the interpolation formula, Eq. (9), to the function $G(\theta)$ leads to the second quadrature formula

$$I\approx\frac{1}{R}\sum_{r=1}^{R}(-1)^r\sin\bar{\theta}_r G(\bar{\theta}_r)\times\int_0^\pi\frac{\cos R\theta}{\cos\bar{\theta}_r-\cos\theta}d\theta=\frac{\pi}{R}\sum_{r=1}^{R}G(\bar{\theta}_r) \qquad (13)$$

This formula may be called "rectangular rule" in comparison with the trapezoidal rule.

It will be instructive to consider the relation between these formulae and the quadrature formulae of Gaussian type for integrals of the form

$$J=\int_{-1}^{1}W(x)f(x)dx \qquad (14)$$

where $W(x)$ is a weight function. It is shown in Appendix A that, by the substitution of $x=-\cos\theta$, Eqs. (12) and (13) reduce to the quadrature formulae of Gaussian type with the weight functions $W(x)=(1-x^2)^{1/2}$ and $W(x)=(1-x^2)^{-1/2}$ respectively. The quadrature formulae of Gaussian type are exact when the function $f(x)$ is a polynomial of degree not in excess of $2R-1$.[11] Therefore, Eqs. (12) and (13) hold exact when $\bar{G}(\theta)/\sin\theta$ and $G(\theta)$, respectively, are polynomials in $(-\cos\theta)$ of degrees not in excess of $2R-1$.

3. NLR METHOD

The integral equation of the subsonic steady lifting-surface theory is written in the form

$$\alpha(x, y)=\frac{1}{8\pi}\int_{-s}^{s}\int_{x_l(y')}^{x_t(y')}l(x', y')K(x, y; x', y')dx'dy' \qquad (15)$$

where α is the downwash angle (the downwash as a fraction of stream velocity), l the wing loading (the lift per unit area) as a fraction of stream dynamic pressure, s the semispan, and x_l and x_t the coordinates of leading and trailing edges respectively. Since the kernel K has a singularity of the form $(y-y')^{-2}$, Mangler's principal value[1,13] must be taken in the integral with respect to y'.

In order to solve Eq. (15) for the unknown function l, the latter is approximated by a superposition of known chordwise loading functions $\Psi_q(\phi')$ as

$$l(x', y')\approx\frac{8s}{\pi c(y')}\sum_{q=1}^{N}\Gamma_q(\eta')\Psi_q(\phi') \qquad (16)$$

where ϕ' is a chordwise angular variable whose relation with x' is given by

$$x'=x_l(y')+\frac{1}{2}c(y')(1-\cos\phi') \qquad (17)$$

c is the cord length, and $\eta'=y'/s$. The coefficients $\Gamma_q(\eta')$ in Eq. (16) are unknown. By putting $\eta'=-\cos\theta'$ and by applying Eq. (1) to the functions Γ_q, Eq. (16) becomes

$$l(x',y')\approx\frac{8s}{\pi c(y')}\sum_{q=1}^{N}\Psi_q(\phi')\sum_{r=1}^{m}\Gamma_q(\eta_r)f_r{}^m(\theta') \qquad (18)$$

where

$$\eta_r=-\cos\theta_r, \qquad \theta_r=\frac{r\pi}{m+1} \qquad (19)$$

Corresponding to the approximation by Eq. (18), Eq. (15) is made be satisfied only at a finite number of points. These points are the so called Multhopp collocation points, whose positions are defined by the m sections

$$\left.\begin{aligned}&\eta_\nu=y_\nu/s=-\cos\theta_\nu\\&\theta_\nu=\frac{\nu\pi}{m+1} \qquad (\nu=1,2,\cdots,m)\end{aligned}\right\} \qquad (20)$$

and by the N points on each sections

$$\left.\begin{aligned}&x_{p\nu}=x_l(y_\nu)+\frac{1}{2}c(y_\nu)(1-\cos\phi_p)\\&\phi_p=\frac{2\pi p}{2N+1} \qquad (p=1,2,\cdots,N)\end{aligned}\right\} \qquad (22)$$

Substituting Eq. (18) into Eq. (15), transforming the integration variables from x' and y' to ϕ' and θ' respectively, and further substituting the coordinates of collocation points, we have

$$\alpha(x_{p\nu},y_\nu)=-\frac{1}{2\pi}\sum_{q=1}^{N}\sum_{r=1}^{m}\Gamma_q(\eta_r)\times\int_0^\pi\frac{f_r{}^m(\theta')F_q(x_{p\nu},\eta_\nu;\eta')\sin\theta'}{(\eta_\nu-\eta')^2}d\theta'$$
$$(\nu=1,2,\cdots,m;\ p=1,2,\cdots,N) \qquad (23)$$

where the functions F_q are called influence functions and are given by

$$F_q(x,\eta;\eta')=-\frac{1}{\pi}\int_0^\pi(y-y')^2\times K(x,y;x',y')\Psi_q(\phi')\sin\phi' d\phi' \qquad (24)$$

$m\times N$ equations given by Eq. (23) with the $m\times N$ collocation points $(x_{p\nu},y_\nu)$ constitute a system of linear simultaneous algebraic equations for $m\times N$ unknowns $\Gamma_q(\eta_r)$. If we write as $\alpha(x_{p\nu},y_\nu)=\alpha_{p\nu}$, $\Gamma_q(\eta_r)=\Gamma_{qr}$, and

$$A_{qr}(p,\nu)=-\frac{1}{2\pi}\times\int_0^\pi\frac{f_r{}^m(\theta')F_q(x_{p\nu},\eta_\nu;\eta')\sin\theta'}{(\eta_\nu-\eta')^2}d\theta' \qquad (25)$$

then Eq. (23) becomes

$$\alpha_{p\nu}=\sum_{q=1}^{N}\sum_{r=1}^{m}A_{qr}(p,\nu)\Gamma_{qr} \qquad (26)$$

Zandbergen et al. of NLR[5] (National Aerospace Laboratory, The Netherlands) presented an improved method for evaluating the integral in Eq. (25). Let us derive the resultant expressions for the coefficients $A_{qr}(p,\nu)$ by this NLR method in a somewhat simpler way. Since the influence functions F_q contain logarithmic singularities,[1] the lowest-order terms of them are removed as

$$P_q(x,\eta;\eta')=F_q(x,\eta;\eta')-C_q(x,\eta)(\eta'-\eta)^2\log|\eta'-\eta| \qquad (27)$$

Further the regularized influence functions

$$R_q(x,\eta;\eta')=\frac{\sin\theta'}{(\eta'-\eta)^2}\{P_q(x,\eta;\theta')-P_q(x,\eta;\eta)-(\eta'-\eta)P_q'(x,\eta;\eta)\} \qquad (28)$$

are introduced, where $P_q'(x,\eta;\eta)$ means $[\partial P_q(x,\eta;\eta')/\partial\eta']_{\eta'=\eta}$. Although the term "regularized influence function" seems to be known together with the NLR method, it would be of some interest to note that its concept was suggested originally by Multhopp[1] as stated in the introduction and also that P. T. Hsu[2] derived his ingenious integration techinique using a similar concept.*

By substituthng Eqs. (27) and (28) into Eq. (25), we have

$$A_{qr}(p,\nu)=B_{qr}(p,\nu)+b_{\nu r}P_q(x_{p\nu},\eta_\nu;\eta_\nu)+c_{\nu r}P_q'(x_{p\nu},\eta_\nu;\eta_\nu)+d_{\nu r}C_q(x_{p\nu},\eta_\nu) \quad (29)$$

where the coefficients $B_{qr}(p,\nu)$, $b_{\nu r}$, $c_{\nu r}$, and $d_{\nu r}$ are defined by

$$B_{qr}(p,\nu)=-\frac{1}{2\pi}\int_0^\pi f_r{}^m(\theta')R_q(x_{p\nu},\eta_\nu;\eta')d\theta' \quad (30)$$

$$\left.\begin{aligned} b_{\nu r}&=-\frac{1}{2\pi}\int_0^\pi \frac{f_r{}^m(\theta')\sin\theta'}{(\eta'-\eta_\nu)^2}d\theta' \\ c_{\nu r}&=-\frac{1}{2\pi}\int_0^\pi \frac{f_r{}^m(\theta')\sin\theta'}{\eta'-\eta_\nu}d\theta' \\ d_{\nu r}&=-\frac{1}{2\pi}\times\int_0^\pi f_r{}^m(\theta')\log|\eta_\nu-\eta'|\sin\theta' d\theta' \end{aligned}\right\} \quad (31)$$

In the first and second integrals in Eqs. (31), Mangler's and Cauchy's principal values, respectively, must be taken. Analytic forms for the coefficients $b_{\nu r}$, $c_{\nu r}$, and $d_{\nu r}$ have been given in Refs. 5 and 6.**

As to the integral in Eq. (30), its integrand is seen to be of the same ature as that in Eq. (10). Therefore the application of the quadrature formula of Eq. (12) yields

$$B_{qr}(p,\nu)=\sum_{\lambda=1}^{\Lambda} a_{r\lambda}R_q(x_{p\nu},\eta_\nu;\eta_\lambda) \quad (32)$$

where

$$a_{r\lambda}=-\frac{f_r{}^m(\theta_\lambda)}{2(\Lambda+1)} \quad (33)$$

$$\left.\begin{aligned} \eta_\lambda&=-\cos\theta_\lambda, \qquad \theta_\lambda=\frac{\lambda\pi}{\Lambda+1} \\ \Lambda&=a(m+1)-1 \end{aligned}\right\} \quad (34)$$

a being a positive integer.*

Eqs. (29) to (34) are essentially the same as the corresponding results of the NLR method. However, the above derivation of Eq. (32) is not only simpler than the NLR method but also enables us to make some discussion about accuracy. By the consideration given at the end of the last section, it is possible to say that Eq. (32) holds exact provided that the functions $f_r{}^m(\theta')R_q(x_{p\nu},\eta_\nu;\eta')/\sin^2\theta'$ are polynomials in $\eta'=-\cos\theta'$ of degree not in excess of $2\Lambda-1$. Since the functions $f_r{}^m(\theta')/\sin\theta'$ are seen to be polynomials of degree $m-1$ from Eqs. (A.9) and (A.3) in Appendix A, Eq. (32) holds exact provided that the functions $R_q(x_{p\nu},\eta_\nu;\eta')/\sin\theta'$ are polynomials of degree not in excess of

$$(2\Lambda-1)-(m-1)=(2a+1)(m+1)-1$$

4. DISPUTABLE POINTS

Comparisons of the NLR method with the method of Ref. 3 (NPL method) seem to show that the former is somewhat superior to the latter.[8,9] An extension of the NLR method to the case of oscillating wings was made by Lehrian and Garner[6] as stated in the introduction. However, there may still be pointed out at least the following two disputable points.

Point 1: In the regularized influence functions $R_q(x_{p\nu},\eta_\nu;\eta_\lambda)$ in Eq. (32), there will occur the coincidences $\eta_\lambda=\eta_\nu$ for certain values of λ and ν. Comparing Eq (20) with Eq. (34), we see that these will occur when $\lambda=a\nu$ and that there will always be such values of λ and ν. At these coincident points, the values of $R_q(x_{p\nu},\eta_\nu;\eta_\nu)$ cannot be obtained from Eq. (28), but instead should be computed by

$$R_q(x_{p\nu},\eta_\nu;\eta_\nu)=\frac{1}{2}\sin\theta_\nu[\partial^2P_q(x_{p\nu},\eta_\nu;\eta')/\partial\eta'^2]_{\eta'=\eta_\nu} \quad (35)$$

* The integrand of the first integral on the right-hand side of his Eq. (5.17) becomes a similar form to Eq. (28) above by the substitution of his Eqs. (5.15) and (5.16). Williams[12] used an expression exactly of the same form as Eq. (28) to derive Hsu's integration formula.

** The coefficients $b_{\nu r}$, $c_{\nu r}$, and $d_{\nu r}$ correspond, respectively, to $\rho_{\nu r}$, $\sigma_{\nu r}$, and $\tau_{\nu r}$ in Ref. 6 and to $-\varepsilon_{\nu n}\sin\theta_n/(2\sin\theta_\nu)$, $-\zeta_{\nu n}/2$, and $-s_{\nu n}/2$ in Ref. 5. Incidentally the coefficients $b_{\nu r}$ are essentially equivalent to the Multhopp coefficients $b_{\nu n}$.

* The coefficients $a_{r\lambda}$ correspond to $k_{r\lambda}$ in Ref. 6 and to $-\gamma_{n\lambda}/[2(\Lambda+1)]$ in Ref. 5.

It has been pointed out in Ref. 6 that a vast computing time is needed to obtain the values of $\partial^2 P_q/\partial\eta'^2$ in the case of oscillating wings, although in the case of steady wings there are no special difficulties about this.[5]

Point 2: Garner and Miller[9] computed the downwash α for steady rectangular wings by specifying the wing loading l. According to them, the convergence in $\alpha(x, y)$ by the NPL method with respect to the parameter a in Eq. (34) deteriorates unlimitedly as the point (x, y) approaches the leading or the trailing edges. This seems to be especially serious near the leading edge. Also in the NLR method, circumstances seem to be more or less similar. In computing the values of $A_{qr}(p, \nu)$ of Eq. (25), therefore, there will occur the situation that making the number of chordwise collocation points N large must be accompanied with making the parameter a also large, since as the number N becomes large the collocation points corresponding to $p=1$ and $p=N$ approach the leading and the trailing edges respectively.[14] It has been suggested in Ref. 6 that the parameters N, m, and a should be selected to satisfy the relation $a(m+1)>(2N-4)(1+2A)$ in order to obtain about three-figure accuracy in the generalized forces, A being the aspect ratio. For example, for $A=8$ and $N=5$, we have the number of spanwise integration points $\Lambda=a(m+1)-1>101$ according to this criterion. Since a considerable time will be consumed to compute values of the regularized influence functions especially in the case of oscillating wings, as small a number of spanwise integration points as possible will be requested.

The reason why the convergence in the downwash α deteriorates near the leading and the trailing edges may be attributed to the fact that the effect of removing the logarithmic singularities from the influence functions by Eq. (27) will diminish in these areas.[14] In the case of steady wings, the influence functions $F_q(x, \eta; \eta')$ are expanded, when $|\eta-\eta'|$ is small, as[1]

$$F_q(x, \eta; \eta')$$
$$=F_q(x, \eta; \eta)+a_1 Y^2+a_2 Y^4+\cdots$$
$$+\frac{2}{\pi}\log Y\left(-Y^2\frac{d\Psi_q}{dX_0}\bigg|_{\phi'=\phi}+\frac{Y^4}{8}\frac{d^3\Psi_q}{dX_0^3}\bigg|_{\phi'=\phi}-\cdots\right) \quad (36)$$

where

$$\left.\begin{aligned} X_0&=\frac{x'-x_l(y')}{c(y')}=\frac{1}{2}(1-\cos\phi')\\ Y&=\frac{\beta s|\eta-\eta'|}{c(y')}\\ \frac{1}{2}(1-\cos\phi)&=\frac{x-x_l(y')}{c(y')}=X \end{aligned}\right\} \quad (37)$$

and $\beta=(1-M^2)^{1/2}$, M being the Mach number. The last term of Eq. (27) has been taken from the lowest-order term obtained by expanding the term containing $Y^2\log Y$ in Eq. (36) with respect to η' in the neighbourhood of $\eta'=\eta$. As will be shown in Appendix B, however, the region of Y where Eq. (36) converges becomes smaller and smaller as x approaches $x_l(y')$ or $x_t(y')$.

5. DEVICES FOR IMPROVEMENT

Let us consider here some possible devices for improvement to cope with the two points discussed in the last section.

A device for point 1: In Ref. 1, Multhopp simply borrowed the coordinates of the collocation sections, η_ν, from his method for solving the lifting-line equation,[10] in which there was not shown so much essentiality to define the coordinates η_ν by Eq. (20). That these coordinates are optimum in a sense was shown first by Hsu[2] and later by Davies.[15] However, since it may be possible to select a different weight function in deriving optimum coordinates of the collocation sections, we can see that the coordinates η_ν defined by Eq. (20) are not the only optimum ones. Similary, since the coordinates of spanwise integration points depend on a quadrature formula applied, the coordinates η_λ defined by Eq. (34) are also not the only optimum ones. It may therefore be possible to find optimum collocation sections and spanwise integration points so that the coincidences $\eta_\lambda=\eta_\nu$ do not occur for any values of ν and λ.

Let us retain here the collocation sections defined by Eq. (20), and apply the quadrature formula of Eq. (13) instead of Eq. (12) to Eq. (30). Then we have

$$B_{qr}(p,\nu)=\sum_{\lambda=1}^{\Lambda_1}\bar{a}_{r\lambda}R_q(x_{p\nu},\eta_\nu;\bar{\eta}_\lambda) \quad (38)$$

$$\bar{a}_{r\lambda}=-\frac{f_r^m(\bar{\theta}_\lambda)}{2\Lambda_1} \quad (39)$$

$$\bar{\eta}=-\cos\bar{\theta}_\lambda, \qquad \bar{\theta}_\lambda=\frac{(2\lambda-1)\pi}{2\Lambda_1} \quad (40)$$

If we choose, as the number of spanwise integration points,

$$\Lambda_1=a(m+1) \quad (41)$$

then the angular coordinates $\bar{\theta}_\lambda$ do not coincide with θ_ν defined by Eq. (20) for any values of ν and λ, since

$$\theta_\lambda=(2\lambda-1)\pi/[2a(m+1)]$$

There will not, therefore, occur the coincidences $\bar{\eta}_\lambda=\eta_\nu$ for any values of ν and λ.* Incidentally, when $a=1$, Eq. (40) gives the same spanwise integration points as those of Hsu.[2]

A device for point 2: In Fig. 1 are shown variations of the regularized influence function with $q=1$ for a rectangular wing of aspect ratio 6 in incompressible flow in the form $R_1(x,0;\eta')/[R_1(x,0;0)\sin\theta']$, where $\cot(\phi'/2)$ has been chosen as the chordwise loading function $\Psi_1(\phi')$. Since the curves are symmetric about the line $\eta'=0$, only left or right halves of them have been plotted. We can see that the regularized influence function $R_1(x,\eta;\eta')$ shows relatively small but undesirable sharp variations in the vicinity of $\eta'=\eta(=0)$ when $x-x_l$ or x_t-x is small. This is clearly the immediate cause, in the NLR method, of the necssity of making the number of integration points Λ larger than the number of abscissae m for interpolating the spanwise loading functions Γ_q by introducing the parameter a to evaluate the itnegral of Eq. (30). A more remote cause may be attributed to the diminution of the effect of removing the logarithmic singularities from the influence functions near the leading and the trailing edges as explained in the last section.

It is not economical to densely distribute the integration points over the whole span of a wing to cope with this difficulty, since the regularized influence functions show the sharp variations only in the vicinity of $\eta'=\eta$. For the purpose of distributing the integration points densely only in the vicinity of $\eta'=\eta$, let us apply the idea of the method of arbitrary collocation points* proposed by Kondo[17] and extended by Hanaoka.[18] We introduce monotonously increasing differentiable functions $F_\nu(\varphi)$ defined in the interval $[-\delta,\pi+\delta]$, where $\delta\geq0$. As shown in Fig. 2, the functions $F_\nu(\varphi)$ satisfy

$$\left.\begin{aligned}&F_\nu(-\delta)=0\\&F_\nu(\theta_\nu)=\theta_\nu\\&F_\nu(\pi+\delta)=\pi\end{aligned}\right\} \quad (42)$$

and have small derivatives $F_\nu'(\varphi)$ near $\varphi=\theta_\nu$, although $F_\nu'(\varphi)\geq0$ by the definition. If we transform the integration variable of the integral in Eq. (30) from θ' to Φ by the transformations

$$\left.\begin{aligned}&\theta'=F_\nu(\varphi)\\&\varphi=\left(\frac{\pi+2\delta}{\pi}\right)\Phi-\delta\end{aligned}\right\} \quad (43)$$

then we have

$$B_{qr}(p,\nu)=-\frac{\pi+2\delta}{2\pi^2}\times\int_0^\pi f_r^m(\theta')R_q(x_{p\nu},\eta_\nu;\eta')F_\nu'(\varphi)d\Phi \quad (44)$$

* The same spanwise integration points as those given by Eqs. (40) and (41) were used by Davies[16] who showed the occurence of the same sort of cancellation as that in Hsu's method. This part of the present work was done in 1976 independently of Davies'. The above cancellation was proved also by the present author.

* This method was originally devised in connection with the lifting-line theory to distribute the collocation and integration points densely over such regions as near the control-surface edge where the circulation varies sharply.

If the integrand of the integral in Eq. (44) is denoted by $G(\Phi)$, we can apply the interpolation of Eq. (9) to it, since $dG/d\Phi$ vanishes at $\Phi=0$ and $\Phi=\pi$. In other words, the quadrature fomula of Eq. (13) can be applied to Eq. (44) which becomes

$$B_{qr}(p,\nu)=\sum_{\lambda=1}^{\Lambda_2} a_{r\lambda}{}^{\nu} R_q(x_{p\nu},\eta_\nu;\eta_{\nu\lambda}) \qquad (45)$$

where

$$a_{r\lambda}{}^{\nu}=-\left(\frac{\pi+2\delta}{2\pi\Lambda_2}\right) f_r{}^m(\theta_{\nu\lambda})F_\nu'(\varphi_\lambda) \qquad (46)$$

and

$$\left.\begin{aligned} &\eta_{\nu\lambda}=-\cos\theta_{\nu\lambda}\\ &\theta_{\nu\lambda}=F_\nu(\varphi_\lambda)\\ &\varphi_\lambda=\left(\frac{\pi+2\delta}{\pi}\right)\Phi_\lambda-\delta\\ &\Phi_\lambda=\frac{(2\lambda-1)\pi}{2\Lambda_2} \end{aligned}\right\} \qquad (47)$$

The distribution of the integration points whose coordinates are $\eta_{\nu\lambda}$ should be dense near $\eta'=\eta_\nu$ since we have made $F_\nu'(\varphi)$ small near $\varphi=\theta_\nu$. Let us further set

$$\left.\begin{aligned} &\delta=\frac{h\pi}{m+1}\\ &\Lambda_2=a(m+1+2h) \end{aligned}\right\} \qquad (48)$$

where a is a positive integer as in the NLR method, and h is zero or a positive integer. Then there will not occur the situations $\varphi_\lambda=\theta_\nu$ for any values of ν and λ, since $\varphi_\lambda=(2\lambda-2ah-1)\pi/[2a(m+1)]$. This, in other words, means from Eqs. (42) and (47) that we are free from the coincidences $\eta_{\nu\lambda}=\eta_\nu$ for any values of ν and λ (There may, however, occur the other kind of coincidences $\theta_{\nu\lambda}=\theta_r$). We can thus retain simultaneously the condition of the device for the point 1.

6. RECTANGULAR WINGS SUPPORTING SIMPLE LOADINGS

Lehrian and Garner,[20,9] investigated convergence characteristics of the NPL and NLR methods by computing the downwash at the surface of rectangular wings subjected to simple wing loadings. In order to make a similar investigation, we reduce here the equations discussed above for evaluating the downwash to those for steady rectangular wings in incompressible flow subjected to simple loadings.

In this case, we can put $x_l(y')=0$ and $x_t(y')=c$, c being the chord length. The kernel $K(x,y;x',y')$ is given by

$$K(x,y;x',y')=-\frac{1}{(y-y')^2}\left[1+\frac{x-x'}{\{(x-x')^2+(y-y')^2\}^{1/2}}\right] \qquad (49)$$

It will be convenient to put

$$\xi=\frac{x}{c},\qquad \xi'=\frac{x'}{c} \qquad (50)$$

and

$$\left.\begin{aligned} &\xi=\frac{1}{2}(1-\cos\phi)\\ &\xi'=\frac{1}{2}(1-\cos\phi') \end{aligned}\right\} \qquad (51)$$

The wing loading $l(x',y')$ is assumed to be of the following form consisting of a single term instead of Eq. (16) as

$$l(x',y')=\frac{4A}{\pi}\Gamma(\eta')\Psi(\phi') \qquad (52)$$

where $A=2s/c$ is the aspect ratio. Eq. (23) then reduces to

$$\alpha(\xi,\eta_\nu)=-\frac{1}{2\pi}\int_0^\pi \frac{\Gamma(\eta')F(\xi,\eta_\nu-\eta')\sin\theta'}{(\eta_\nu-\eta')^2}d\theta' \qquad (53)$$

where the chordwise coordinate ξ is left unspecified. The influence function $F(\xi,\eta_\nu-\eta')$ is given by

$$F(\xi,\eta_\nu-\eta')=\frac{1}{\pi}\int_0^\pi\left[1+\frac{\xi-\xi'}{\{(\xi-\xi')^2+(A/2)^2(\eta_\nu-\eta')^2\}^{1/2}}\right]\times\Psi(\phi')\sin\phi'd\phi' \qquad (54)$$

Removing the logarithmic singularity, we get

$$P(\xi,\eta_\nu-\eta')=F(\xi,\eta_\nu-\eta')-C(\xi)(\eta'-\eta_\nu)^2\log|\eta'-\eta_\nu| \qquad (55)$$

The coefficient $C(\xi)$ can be determined from the term containing $Y^2 \log Y$ in Eq. (36) by making use of Eq. (37) as

$$C(\xi) = -\left(\frac{A^2}{\pi \sin \phi}\right) \frac{d\Psi(\phi')}{d\phi'}\bigg|_{\phi'=\phi} \quad (56)$$

From Eq. (54), the influence function $F(\xi, \eta_\nu - \eta')$ is seen to be an even function in $\eta' - \eta_\nu$, and so is $P(\xi, \eta_\nu - \eta')$ from Eq. (55). Therefore

$$\frac{\partial P(\xi, \eta_\nu - \eta')}{\partial \eta'}\bigg|_{\eta'=\eta_\nu} = 0 \quad (57)$$

The regularized influence function then reduces to

$$R(\xi, \eta_\nu - \eta') = \left\{\frac{P(\xi, \eta_\nu - \eta') - P(\xi, 0)}{(\eta' - \eta_\nu)^2}\right\} \sin \theta' \quad (58)$$

where $P(\xi, 0)$ is obtained from Eqs. (54) and (55) as

$$P(\xi, 0) = F(\xi, 0) = \frac{2}{\pi}\int_0^\phi \Psi(\phi') \sin \phi' d\phi' \quad (59)$$

Insertion of Eqs. (55) and (58) to Eq. (53) yields

$$\alpha(\xi, \eta_\nu) = B(\xi, \eta_\nu) + b(\eta_\nu) P(\xi, 0) + d(\eta_\nu) C(\xi) \quad (60)$$

where

$$B(\xi, \eta_\nu) = -\frac{1}{2\pi}\int_0^\pi \Gamma(\eta') R(\xi, \eta_\nu - \eta') d\theta' \quad (61)$$

$$b(\eta_\nu) = -\frac{1}{2\pi}\int_0^\pi \frac{\Gamma(\eta') \sin \theta'}{(\eta' - \eta_\nu)^2} d\theta' \quad (62)$$

and

$$d(\eta_\nu) = -\frac{1}{2\pi}\int_0^\pi \Gamma(\eta') \log|\eta_\nu - \eta'| \sin \theta' \mathrm{d}\theta' \quad (63)$$

In the numerical examples presented in the next section, $\Gamma(\eta')$ and $\Psi(\phi')$ are specified as

$$\Gamma(\eta') = (1 - \eta'^2)^{1/2} = \sin \theta' \quad (64)$$

and

$$\Psi(\phi') = \cot\left(\frac{\phi'}{2}\right) \quad (65)$$

Then the integrals in Eqs. (59), (62), and (63) are evaluated analytically as

$$P(\xi, 0) = \frac{2}{\pi}(\phi + \sin \phi) \quad (66)$$

$$b(\eta_\nu) = \frac{1}{2} \quad (67)$$

and

$$d(\eta_\nu) = \frac{1}{8}(2 \log 2 - \cos 2\theta_\nu) \quad (68)$$

where we have referred to p. 42 of Ref. 1 and Appendix I of Ref. 4 in deriving Eqs. (67) and (68) respectively.

The evaluation of $B(\xi, \eta_\nu)$ depends on the methods discussed above.

First, if the quadrature formula of Eq. (12) is applied to Eq. (61) with Eq. (64), we get the evaluation by the NLR method as

$$B(\xi, \eta_\nu) = -\frac{1}{2(\Lambda+1)}\sum_{\lambda=1}^{\Lambda}(\sin \theta_\lambda) R(\xi, \eta_\nu - \eta_\lambda) \quad (69)$$

Secondly, the application of the quadrature formula of Eq. (13) leads to the evaluation by the method proposed as the device for point 1 as

$$B(\xi, \eta_\nu) = -\frac{1}{2\Lambda_1}\sum_{\lambda=1}^{\Lambda_1}(\sin \bar{\theta}_\lambda) R(\xi, \eta_\nu - \bar{\eta}_\lambda) \quad (70)$$

Let us call this method "Method 1".

Finally, transforming the integration variable from θ' to Φ by Eqs. (43), and applying Eq. (13), we have the evaluation by the method proposed as the device for point 2 as

$$B(\xi, \eta_\nu) = -\frac{1}{2a(m+1)}\sum_{\lambda=1}^{\Lambda_2} \sin \theta_{\nu\lambda} \times R(\xi, \eta_\nu - \eta_{\nu\lambda}) F_\nu'(\varphi_\nu) \quad (71)$$

where we have also used the relations of Eqs. (48). We shall call this method "Method 2".

The transforming functions $F_\nu(\varphi)$ tested in the examples are of the following two kinds. The first kind is defined by

$$F_\nu^{(1)}(\varphi)=\begin{cases}\theta_\nu-\dfrac{(\theta_\nu-\varphi)^2}{\theta_\nu} & (0\leq\varphi\leq\theta_\nu)\\ \theta_\nu+\dfrac{(\varphi-\theta_\nu)^2}{\pi-\theta_\nu} & (\theta_\nu\leq\varphi\leq\pi)\end{cases} \quad (72)$$

in which δ has been set equal to zero. The derivatives of $F_\nu^{(1)}(\varphi)$ are given by

$$F_\nu^{(1)\prime}(\varphi)=\begin{cases}\dfrac{2(\theta_\nu-\varphi)}{\theta_\nu} & (0\leq\varphi\leq\theta_\nu)\\ \dfrac{2(\varphi-\theta_\nu)}{\pi-\theta_\nu} & (\theta_\nu\leq\varphi\leq\pi)\end{cases} \quad (73)$$

The second kind is defined by

$$F_\nu^{(2)}(\varphi)=\begin{cases}\theta_\nu-\dfrac{\theta_\nu(\theta_\nu-\varphi)^3}{(\theta_\nu+\delta)^3} & (-\delta\leq\varphi\leq\theta_\nu)\\ \theta_\nu+\dfrac{(\pi-\theta_\nu)(\varphi-\theta_\nu)^3}{(\pi+\delta-\theta_\nu)^3} & (\theta_\nu\leq\varphi\leq\pi+\delta)\end{cases} \quad (74)$$

The derivatives of $F_\nu^{(2)}(\varphi)$ are given by

$$F_\nu^{(2)\prime}(\varphi)=\begin{cases}\dfrac{3\theta_\nu(\theta_\nu-\varphi)^2}{(\theta_\nu+\delta)^3} & (-\delta\leq\varphi\leq\theta_\nu)\\ \dfrac{3(\pi-\theta_\nu)(\varphi-\theta_\nu)^2}{(\pi+\delta-\theta_\nu)^3} & (\theta_\nu\leq\varphi\leq\pi+\delta)\end{cases} \quad (75)$$

7. NUMERICAL EXAMPLES AND DISCUSSIONS

The downwash angle at the surface of a steady rectangular wing of aspect ratio 6 in incompressible flow has been computed by following the various schemes defined in the last section. The wing loading $l(x', y')$ has been specified as

$$l(x', y')=\frac{4A}{\pi}\sin\theta'\cot\left(\frac{\phi'}{2}\right) \quad (76)$$

The influence function $F(\xi, \eta_\nu-\eta')$, Eq. (54), has been evaluated by making use of the method of Ref. 3. Since $|\eta_\nu-\eta_{\nu\lambda}|$ can take very small values in Method 2, it has been necessary to evaluate the influence function in double precision to obtain accurate values of the regularized influence function, Eq. (58), for small values of $|\eta_\nu-\eta_{\nu\lambda}|$. Some values of the regularized influence function for $\eta_\nu=0$ are given in Table 1 in the form $R(\xi, -\eta')/\{R(\xi, 0)\sin\theta'\}$. This table corresponds to Fig. 1. The values of $R(\xi, 0)$ have been obtained from[9]

$$R(\xi, 0)=\left(\frac{A^2}{4\pi}\right)\xi^{-3/2}(1-\xi)^{-1/2}\times\left[\frac{3}{2}-2\xi-\log\left\{\frac{16\xi(1-\xi)}{A}\right\}\right] \quad (77)$$

The computed downwash angles α by the various methods are presented in Tables 2 to 5 with various numbers of spanwise integration points Λ, and for various values of ξ and some values of η_ν. These α for some values of ξ and η_ν are plotted against Λ in Figs. 3 to 5.

The results of Method 1 for $\eta_\nu=0$ are given in Table 2. Convergence of α with respect to Λ for $\xi=0.5$ is seen to be fairly good, that is, convergence down to four decimal places has been achieved with $\Lambda=47$. Convergence for $\xi=0.05$, however, is rather poor, which is clearly due to the reason explained in Sections 4 and 5.

The results for $\xi=0.05$ and 0.15 in Table 2 are compared with those by the NLR method in Figs. 3(a) to (b). The results of the latter method have been taken from Ref. 20 and contain those with Λ both even and odd. We can see that the results of Method 1 agree very well with those of the NLR method with Λ even. This will be attributed to approximately the same distributions of spanwise integration points near $\eta_\nu=0$ in the both methods in which no integration point is located at $\eta_\nu=0$. In the NLR method with Λ odd, on the other hand, there is located an integration point at $\eta_\nu=0$. It should be noted that, in the original NLR method, only cases with Λ odd are possible when the centre section is one of the collocation sections, because, then, the number of collocation sections m is odd and therefore $\Lambda=a(m+1)-1$ is also odd.

The results of Method 2 for $\eta_\nu=0$ using the transforming functions of the first kind $F_\nu^{(1)}(\varphi)$ are shown in Table 3. Only slight improvement in convergence near the leading and trailing edges is observed compared with the results of Method 1. It may be instructive to note that the slopes of

$F_\nu^{(1)\prime}(\varphi)$ are discontinuous at $\varphi=\theta_\nu$.

In Tables 4(a) to (c), the results of Method 2 using the transforming functions of the second kind $F_\nu^{(2)}(\varphi)$ with $\delta=0$ are presented for $\eta_\nu=0$, 0.5, and 0.965926 ($\theta_\nu=6\pi/12$, $8\pi/12$, and $11\pi/12$). Improvement in convergence for $\eta_\nu=0$ and 0.5 is remarkable. Especially, for $\eta_\nu=0$, convergence down to five or six decimal places has been achieved with $\Lambda=47$ over the greater part of the chord, that is, at least from $\xi=0.05$ to $\xi=0.95$. For $\eta_\nu=0.965926$, however, we hardly observe any improvement by this method.

The results for $\xi=0.05$ and $\eta_\nu=0$ and 0.965926 by Method 1, Method 2 using $F_\nu^{(1)}(\varphi)$, and Method 2 using $F_\nu^{(2)}(\varphi)$ with $\delta=0$ are compared in Figs. 4(a) and (b). We can see rather adverse effects of these $F_\nu(\varphi)$ for $\eta_\nu=0.965926$. This may be thought natural if we notice that both $F_\nu^{(1)\prime}(\varphi)$ and $F_\nu^{(2)\prime}(\varphi)$ with $\delta=0$ make sharp variations when η_ν is located near the wing tips, $\eta=\pm1$.

The purpose of expanding the interval of φ by introducing δ as in Eqs. (42) is to cure this difficulty. The results of Method 2 using $F_\nu^{(2)}(\varphi)$ with $\delta=\pi/12$, $2\pi/12$, and $3\pi/12$ for $\eta_\nu=0.965926$ are given in Tables 5 (a) to (c). Improved convergence by the introduction of δ is clearly seen. If we take into account the fact that the downwash angle for the present wing loading becomes $-\infty$ at the leading tip corner,[9] the results for $\xi=0.05$ are thought to be satisfactory. The results for $\xi=0.05$ are compared with those of Method 1 in Fig. 5. Convergence with $\delta=2\pi/12$ ($h=2$ in Eqs. (48)) is seen to be the best in the present example.

In the final table, Table 6, the results of Method 2 using $F_\nu^{(2)}(\varphi)$ with $\delta=2\pi/12$ and with $\Lambda=47$ are given for various values of ξ and η_ν. Some of the results obtained by Ray and Miller[21] are also shown for comparison. We can see that the present results for $\eta_\nu=0$ and 0.5 agree with those by Ray and Miller down to at least five decimal places.

8. CONCLUSIONS

Two disputable points in the spanwise integration in the NLR method have been discussed, and devices for improvement to cope with these points have been proposed. The downwash at the surface of a steady rectangular wing in incompressible flow subjected to a simple wing loading has been computed to examine effectiveness of the proposed devices, that is, Method 1 and Method 2. The following conclusions can be deduced from the numerical results.

(1) In Method 1, the values of the regularized influence functions at the coincident spanwise coordinates $R_q(x_{p\nu}, \eta_\nu; \eta_\nu)$ need not be computed. Convergence characteristics of the computed downwash angles with respect to the number of spanwise integration points Λ by Method 1 are nearly the same as those by the NLR method with Λ even. Thus, Method 1 makes it possible to reduce largely the computing time in cases of the oscillating wing with no losses in accuracy.

(2) Improvement in convergence by Method 2 using the transforming functions of the first kind $F_\nu^{(1)}(\varphi)$ compared with Method 1 is only slight.

(3) Remarkable improvement in convergence is obtained by Method 2 using the transforming functions of the second kind $F_\nu^{(2)}(\varphi)$ with $\delta=0$ except for η_ν near the wing tips. The adverse effects at η_ν near the wing tips are cured by expanding the region of φ by 2δ.

(4) The downwash angles for $\eta_\nu=0$ and 0.5 computed by Method 2 using $F_\nu^{(2)}(\varphi)$ with $\delta=2\pi/12$ and with $\Lambda=47$ agree with those by Ray and Miller down to at least five decimal places.

ACKNOWLEDGEMENT

The author would like to thank members of the study group for the lifting-surface theory for their helpful discussions and cooperation in the numerical calculation. They are Dr. Koichi Hiraoka of Kawasaki Heavy Industries, Ltd., Mr. Tetsutaro Katayama of Shin Meiwa Industry Co., Ltd., Mr. Meguru Yano of Fuji Heavy Industries, Ltd., Mr. Hideki Nomoto of Mitsubishi Heavy Industries, Ltd., Mr. Makoto Hirahara of the Civil Transport Development

Corporation, and Dr. Michihiro Natori of Institute of Space and Aeronautical Science, the University of Tokyo.

REFERENCES

1 Multhopp, H.: Methods for Calculating the Lift Distribution of Wings (Subsonic Lifting-Surface Theory), A.R.C. R. & M. 2884, 1950.

2 Hsu, P. T.: Some Recent Developments in the Flutter Analysis of Low-Aspect-Ratio Wings, Proceedings of the National Specialists Meeting on Dynamics and Aeroelasticity, Inst. Aero. Sci., 1958, pp. 7–26.

3 Garner, H. C. and Fox, D. A.: Algol 60 Programme for Multhopp's Low-Frequency Subsonic Lifting-Surface Theory, A.R.C. R. & M. 3517, 1966.

4 Mangler, K. W. and Spencer, B. F. R.: Some Remarks on Multhopp's Subsonic Lifting-Surface Theory, A.R.C. R. & M. 2926, 1952.

5 Zandbergen, P. J., Labrujere, Th. E., and Wouters, J. G.: A New Approach to the Numerical Solution of the Equation of Subsonic Lifting-Surface Theory, NLR TR G. 49, 1967.

6 Lehrian, Doris E. and Garner, H. C.: Theoretical Calculation of Generalized Forces and Load Distribution on Wings Oscillating at General Frequency in a Subsonic Stream, A.R.C. R. & M. 3710, 1973.

7 Garner, H. C.: Accuracy of Downwash Evaluation by Multhopp's Lifting-Surface Theory, A.R.C. R. & M. 3431, 1964.

8 Garner, H. C., Hewitt, B. L., and Labrujere, T. E.: Comparison of Three Methods for the Evaluation of Subsonic Lifting-Surface Theory, A.R.C. R. & M. 3597, 1968.

9 Garner, H. C. and Miller, G. F.: Analytical and Numerical Studies of Downwash over Rectangular Planforms, Aero. Quart., Vol. XXIII, August, 1972, pp. 169–180.

10 Multhopp, H.: Die Berechnung der Auftriebsverteilung von Tragfluegeln, Luftfahrtforschung, Bd. 15, Nr. 4, June, 1938, pp. 153–169.

11 Kopal, Z.: Numerical Analysis, Chapman & Hall Ltd, 1955.

12 Williams, D. E.: Some Mathematical Methods in Three-Dimensional Subsonic Flutter-Derivative Theory, A.R.C. R. & M. 3302, 1961; also in Manual on Aeroelasticity, Part II.

13 Mangler, K. W.: Improper Integrals in Theoretical Aerodynamics, RAE Rept. Aero. 2424, 1951.

14 Jordan, P. F.: Remarks on Applied Subsonic Lifting-Surface Theory, WGLR Jahrbuch, 1967, pp. 192–210.

15 Davies, D. E.: Calculation of Unsteady Generalized Airforces on a Thin Wing Oscillating Harmonically in Subsonic Flow, A.R.C. R. & M. 3409, 1963.

16 Davies, D. E.: Theoretical Determination of Subsonic Oscillatory Airforce Coefficients, RAE TR 76059, 1976.

17 Kondo, K.: On the Practical Method for Solving the Integral Equation with a Singular Kernel
$$K(\eta)\varphi(\eta)+1/(2\pi)\int_{-1}^{1}\varphi(\eta')/(\eta-\eta')d\eta'=g(\eta),$$
in Japanese, Oyo Sugaku Rikigaku (Applied Mathematics and Mechanics), Vol. 1, Nos. 6/7, 1947.

18 Hanaoka, T.: Problems in Numerical Methods for Solving Lifting-Surface Theory, in Japanese, unpublished report, 1975.

19 Ashley, H.: Some Considerations Relative to the Prediction of Unsteady Air Loads on Lifting Configurations, J. Aircraft, Vol. 8, No. 10, 1971, pp. 747–756.

20 Lehrian, Doris E. and Garner, H. C.: Convergence of Current Routines for Evaluating Downwash at a Lifting Surface, NPL Aero. Note 1095, 1970.

21 Ray, Valerie A. and Miller, G. F.: Numerical Evaluation of the Downwash Integral for a Lifting Rectangular Planform, NPL Maths. 90, 1970.

Appendix A

QUADRATURE FORMULAE OF GAUSSIAN TYPE

The quadrature formula of Gaussian type for the integral

$$J=\int_{-1}^{1} W(x)f(x)dx \qquad \text{(A1)}$$

with the weight function $W(x)$ is obtained by applying the Lagrangian interpolation formula[11]

$$f(x)\approx \sum_{r=1}^{R} f(x_r)l_r{}^R(x) \qquad \text{(A2)}$$

to the function $f(x)$. The interpolation coefficients or the interpolation polynomials $l_r{}^R(x)$ are given by

$$l_r{}^R(x)=\frac{p_R(x)}{(x-x_r)p_R'(x_r)} \qquad \text{(A3)}$$

where $p_R(x)$ is an orthogonal polynomial of degree R satisfying the orthogonality conditions

$$\int_{-1}^{1} W(x)p_R(x)x^k dx=0$$
$$k=0,1\ 2,\cdots,R-1 \qquad \text{(A4)}$$

The abscissae x_r are the zeros of the polynomial $p_R(x)$. If we put $x=-\cos\theta$, Eqs. (A1) and (A4) reduce respectively to

$$J=\int_0^{\pi} W(-\cos\theta)f(-\cos\theta)\sin\theta d\theta \qquad \text{(A5)}$$

and

$$\int_0^{\pi} W(-\cos\theta)p_R(-\cos\theta)\sin(k+1)\theta d\theta=0$$
$$k=0,1,2,\cdots,R-1 \qquad \text{(A6)}$$

Let us choose here the two functions $(1-x^2)^{1/2}$ and $(1-x^2)^{-1/2}$ as the weight function $W(x)$, and consider relations between the Gaussian type formulae for these weight functions and the quadrature formulae discussed in Section 2.

We first put $W(x)=(1-x^2)^{1/2}=\sin\theta$. In this case, a polynomial of degree R in $x=-\cos\theta$ satisfying Eq. (A6) is given by

$$p_R(x)=\frac{\sin(R+1)\theta}{\sin\theta} \qquad \text{(A7)}$$

whose zeros are $x_r=-\cos\theta_r$, θ_r being given by Eq. (3). Making use of

$$p_R'(x_r)=\left[\frac{1}{\sin\theta}\frac{dp_R}{d\theta}\right]_{\theta=\theta_r}=\frac{(-1)^r(R+1)}{\sin^2\theta_r} \qquad \text{(A8)}$$

and comparing Eq. (A3) with Eq. (2), we can see that

$$l_r{}^R(x)=\frac{\sin\theta_r}{\sin\theta}f_r{}^R(\theta)=\frac{W(x_r)}{W(x)}f_r{}^R(\theta) \qquad \text{(A9)}$$

If we substitute for $l_r{}^R(x)$ from Eq. (A9) into Eq. (A2), we get

$$W(x)f(x)\approx\sum_{r=1}^{R} W(x_r)f(x_r)f_r{}^R(\theta) \qquad \text{(A10)}$$

We can see that Eq. (A10) is essentially the same interpolation formula as Eq. (1). The quadrature formula Eq. (12) obtained by applying Eq. (1) to $\bar{G}(\theta)$ in Eq. (10) must, therefore, be identical with that obtained by applying Eq. (A10) to $W(x)f(x)$ in Eq. (A5). In other words, Eq. (12) is nothing but a quadrature formula of Gaussian type for the weight function $W(x)=(1-x^2)^{1/2}$.

Secondly, let us put $W(x)=(1-x^2)^{-1/2}=1/\sin\theta$. We can choose, in this case,

$$p_R(x)=\cos R\theta \qquad \text{(A11)}$$

as a polynomial of degree R satisfying Eq. (A6). Zeros of $p_R(x)$ are $x_r=-\cos\bar{\theta}_r$, $\bar{\theta}_r$ being given by Eq. (5). Making use of

$$p_R'(x_r)=\frac{(-1)^r R}{\sin\bar{\theta}_r} \qquad \text{(A12)}$$

and comparing Eq. (A3) with Eq. (6), we see that

$$l_r{}^R(x)=g_r{}^R(\theta) \qquad \text{(A13)}$$

Eq. (A2) then becomes

$$f(x)\approx\sum_{r=1}^{R} f(x_r)g_r{}^R(\theta) \qquad \text{(A14)}$$

which is the same interpolation formula as Eq. (9). The quadrature formula Eq. (13) obtained by applying Eq. (9) to $G(\theta)$ in

Eq. (10) must, therefore, be identical with that obtained by applying Eq. (A14) to $W(x)f(x)\sin\theta=f(x)$ in Eq. (A5), that is, with a quadrature formula of Gaussian type for the weight function $W(x)=(1-x^2)^{-1/2}$.

Appendix B

LOGARITHMIC SINGULARITIES OF INFLUENCE FUNCTIONS

The influence functions $F_q(x,\eta;\eta')$ in the case of steady wings can be expanded, when Y is small, as

$$F_q(x,\eta;\eta')=F_q(x,\eta;\eta)+\frac{2}{\pi}\left\{A_0\Psi_q(\phi)+A_1\frac{d\Psi_q}{dx_0}\bigg|_{\phi'=\phi}+\cdots\right\} \tag{B1}$$

where

$$\left.\begin{aligned} A_0&=1-2X-\{(1-X)^2+Y^2\}^{1/2}\\ &\quad+(X^2+Y^2)^{1/2}\\ A_1&=(1/2)\{(1-X)^2+X^2\}\\ &\quad-(1/2)[(1-X)\{(1-X)^2+Y^2\}^{1/2}\\ &\quad+X\{X^2+Y^2\}^{1/2}]\\ &\quad+(Y^2/2)[\log|1-X\\ &\quad+\{(1-X)^2+Y^2\}^{1/2}|\\ &\quad+\log|X+(X^2+Y^2)^{1/2}|\\ &\quad-2\log|Y|]\cdots \end{aligned}\right\} \tag{B2}$$

Eq. (36) has been derived by expanding the terms containing square roots in the coefficients $A_0, A_1, \cdots$ with respect to Y^2. It will, therefore, be necessary to note the following two points in connection with the convergence of Eq. (36).

First, $\Psi_q(\phi)$, $[d\Psi_q/dX_0]_{\phi'=\phi}$, etc. in Eq. (B1) are generally not bounded. They are the coefficients of the Taylor expansions of the chordwise loading functions $\Psi_q(\phi')$ with respect to X_0 in the neighbourhood of $X_0=X$. While several sets of functions are used as $\Psi_q(\phi')$, they or at least derivatives of them become infinite at the leading and trailing edges. We cannot avoid such infinity in the loading functions because the wing loading $l(x',y')$ as the solution of Eq. (15) has the singularities of the forms $\{x'-x_l(y')\}^{-1/2}$ and $\{x_t(y')-x'\}^{1/2}$ at the leading and trailing edges respectively.[19]

Secondly, for the terms containing square roots in the coefficients $A_0, A_1, \cdots$ to be expanded with respect to Y^2, it is necessary that $Y^2<X^2$ and $Y^2<(1-X)^2$.

By these two reasons, the region of Y in which Eq. (36) converges will become smaller and smaller as X approaches 0 or 1, that is, as x approaches $x_l(y')$ or $x_t(y')$.

Table 1. Values of Regularized Influence Function for $\eta_\nu=0$ in the form $R(\xi,-\eta')/\{R(\xi,0)\sin\theta'\}$

ξ	0.05	0.15	0.50	0.85	0.95
$R(\xi,0)$	911.23	121.89	10.376	8.2949	23.054
η'	$R(\xi,-\eta')/\{R(\xi,0)\sin\theta'\}$				
0.00002454	1.0000	1.0000	1.0000	1.0000	1.0000
0.0006627	1.0007	1.0002	1.0000	1.0001	1.0003
0.003068	1.0086	1.0022	1.0006	1.0011	1.0040
0.008418	1.0279	1.0110	1.0061	1.0061	1.0163
0.01789	1.0217	1.0297	1.0120	1.0188	1.0288
0.03266	0.9509	1.0464	1.0301	1.0390	1.0165
0.05390	0.8413	1.0320	1.0585	1.0572	0.9696
0.08274	0.7260	0.9698	1.0905	1.0592	0.8976
0.1203	0.6184	0.8717	1.1087	1.0363	0.8124
0.1676	0.5213	0.7578	1.0926	0.9868	0.7215
0.2253	0.4342	0.6422	1.0308	0.9113	0.6285
0.2942	0.3560	0.5317	0.9260	0.8114	0.5346
0.3742	0.2858	0.4291	0.7906	0.6911	0.4409
0.4645	0.2227	0.3354	0.6390	0.5568	0.3487
0.5635	0.1666	0.2513	0.4838	0.4168	0.2601
0.6677	0.1173	0.1771	0.3347	0.2794	0.1776
0.7720	0.0753	0.1135	0.2000	0.1527	0.1040
0.8686	0.0412	0.0619	0.0864	0.0443	0.0424
0.9468	0.0162	0.0240	0.0013	−0.0378	−0.0037
0.9934	0.0023	0.0030	−0.0468	−0.0844	−0.0296

Table 2. Downwash Angles $\alpha(\xi,\eta_\nu=0)$ Computed by Method 1

ξ	0.05	0.15	0.3	0.5	0.7	0.85	0.95
Λ	$\alpha(\xi,\eta_\nu=0)$						
11	0.939073	0.331365	0.308992	0.318876	0.324795	0.328096	0.338343
23	0.462092	0.301786	0.314830	0.321764	0.326318	0.328869	0.331441
47	0.302980	0.309833	0.316957	0.322117	0.326517	0.329361	0.330650
71	0.290851	0.312214	0.317142	0.322147	0.326534	0.329429	0.330894
95	0.295923	0.312780	0.317183	0.322155	0.326539	0.329444	0.331049
119	0.301135	0.312962	0.317197	0.322157	0.326540	0.329449	0.331126
143	0.304582	0.313037	0.317203	0.322158	0.326541	0.329451	0.331165

Table 3. Downwash Angles $\alpha(\xi,\eta_\nu=0)$ Computed by Method 2 Using Transforming Functions $F_\nu^{(1)}(\varphi)$

ξ	0.05	0.15	0.3	0.5	0.7	0.85	0.95
A	$\alpha(\xi,\eta_\nu=0)$						
11	0.180160	0.297482	0.312306	0.320605	0.325637	0.328231	0.328306
23	0.276034	0.308523	0.316043	0.321768	0.326312	0.329141	0.330335
47	0.301612	0.311979	0.316920	0.322062	0.326484	0.329376	0.330999
71	0.306406	0.312621	0.317082	0.322116	0.326516	0.329419	0.331120
95	0.308085	0.312845	0.317139	0.322135	0.326527	0.329435	0.331163
119	0.308862	0.312949	0.317165	0.322144	0.326532	0.329442	0.331182
143	0.309284	0.313005	0.317179	0.322149	0.326535	0.329446	0.331193

Table 4. Downwash Angles $\alpha(\xi,\eta_\nu)$ Computed by Method 2 Using Transforming Functions $F_\nu^{(2)}(\varphi)$ with $\delta=0$

(a) $\eta_\nu=0$ $(\theta_\nu=6\pi/12)$

ξ	0.05	0.15	0.3	0.5	0.7	0.85	0.95
A	$\alpha(\xi,\eta_\nu=0)$						
11	0.302414	0.315366	0.317600	0.322483	0.326805	0.329739	0.331548
23	0.310282	0.313153	0.317221	0.322168	0.326549	0.329462	0.331227
47	0.310243	0.313134	0.317212	0.322160	0.326542	0.329455	0.331218
71	0.310242	0.313134	0.317212	0.322160	0.326542	0.329454	0.331217
95	0.310242	0.313134	0.317212	0.322167	0.326542	0.329454	0.331217
119	0.310242	0.313134	0.317212	0.322209	0.326541	0.329454	0.331217
143	0.310242	0.313134	0.317212	0.322160	0.326542	0.329454	0.331217

(b) $\eta_\nu=0.5$ $(\theta_\nu=8\pi/12)$

ξ	0.05	0.15	0.3	0.5	0.7	0.85	0.95
A	$\alpha(\xi,\eta_\nu=0.5)$						
11	0.271849	0.277989	0.284600	0.290833	0.296433	0.300044	0.301964
23	0.274752	0.278899	0.284352	0.290811	0.296370	0.299949	0.302048
47	0.275080	0.278974	0.284380	0.290821	0.296375	0.299954	0.302061
71	0.275107	0.278980	0.284382	0.290824	0.296375	0.299954	0.302062
95	0.275112	0.278981	0.284382	0.290847	0.296375	0.299955	0.302062
119	0.275114	0.278981	0.284382	0.290826	0.296375	0.299955	0.302062
143	0.275114	0.278981	0.284383	0.290838	0.296375	0.299955	0.302062

(c) $\eta_\nu=0.965926$ $(\theta_\nu=11\pi/12)$

ξ	0.05	0.15	0.3	0.5	0.7	0.85	0.95
A	$\alpha(\xi,\eta_\nu=0.965926)$						
11	0.016043	0.114651	0.151615	0.177945	0.193543	0.200218	0.201383
23	0.081183	0.122062	0.153322	0.178415	0.193761	0.200581	0.202737
47	0.092561	0.123847	0.153751	0.178554	0.193838	0.200692	0.203055
71	0.093261	0.123955	0.153778	0.178560	0.193843	0.200699	0.203075
95	0.093384	0.123974	0.153783	0.178561	0.193844	0.200700	0.203078
119	0.093418	0.123979	0.153784	0.178562	0.193845	0.200701	0.203079
143	0.093430	0.123981	0.153785	0.178563	0.193845	0.200701	0.203079

Table 5. Downwash Angles $\alpha(\xi,\eta_\nu=0.965926)$ Computed by Method 2 Using Transforming Functions $F_\nu^{(2)}(\varphi)$

(a) $\delta=\pi/12$ $(h=1)$

ξ	0.05	0.15	0.3	0.5	0.7	0.85	0.95
Λ	$\alpha(\xi,\eta_\nu=0.965926)$						
13	0.085294	0.122899	0.153650	0.178597	0.193904	0.200732	0.202957
27	0.092768	0.123889	0.153768	0.178560	0.193846	0.200700	0.203067
41	0.093300	0.123963	0.153782	0.178562	0.193845	0.200701	0.203077
55	0.093396	0.123976	0.153784	0.178569	0.193845	0.200701	0.203079
69	0.093423	0.123980	0.153785	0.178562	0.193845	0.200701	0.203079
83	0.093433	0.123981	0.153785	0.178562	0.193845	0.200701	0.203079
97	0.093437	0.123982	0.153785	0.178562	0.193845	0.200701	0.203080

(b) $\delta=2\pi/12$ $(h=2)$

ξ	0.05	0.15	0.3	0.5	0.7	0.85	0.95
Λ	$\alpha(\xi,\eta_\nu=0.965926)$						
15	0.094103	0.124185	0.153922	0.178662	0.193931	0.200785	0.203172
31	0.093419	0.123987	0.153791	0.178567	0.193849	0.200705	0.203083
47	0.093436	0.123983	0.153786	0.178564	0.193846	0.200702	0.203080
63	0.093440	0.123983	0.153786	0.178562	0.193845	0.200701	0.203080
79	0.093441	0.123983	0.153785	0.178562	0.193845	0.200701	0.203080
95	0.093442	0.123983	0.153785	0.178564	0.193845	0.200701	0.203080
111	0.093442	0.123983	0.153785	0.178568	0.193845	0.200701	0.203080

(c) $\delta=3\pi/12$ $(h=3)$

ξ	0.05	0.15	0.3	0.5	0.7	0.85	0.95
Λ	$\alpha(\xi,\eta_\nu=0.965926)$						
17	0.094770	0.124297	0.153927	0.178648	0.193915	0.200773	0.203174
35	0.093502	0.123998	0.153793	0.178566	0.193848	0.200705	0.203084
53	0.093453	0.123986	0.153787	0.178565	0.193845	0.200702	0.203081
71	0.093446	0.123984	0.153786	0.178563	0.193845	0.200701	0.203080
89	0.093442	0.123983	0.153786	0.178566	0.193845	0.200701	0.203080
107	0.093443	0.123983	0.153785	0.178562	0.193845	0.200701	0.203080
125	0.093443	0·123983	0.135785	0.178562	0.193845	0.200701	0.203080

Table 6. Downwash Angles $\alpha(\xi,\eta_\nu)$ Computed by Method 2 Using Transforming Functions $F_\nu^{(2)}(\varphi)$ with $\delta=2\pi/12$ and with Number of Spanwise Integration Points $\Lambda=47$

η_ν	0.0	0.258819	0.5	0.707107	0.866025	0.965926	0.0	0.5
ξ	$\alpha(\xi,\eta_\nu)$ Present method						$\alpha(\xi,\eta_\nu)$ Ref. 21	
0.05	0.310243	0.301365	0.275103	0.232290	0.172950	0.093436		
0.1	0.311705	0.302936	0.277070	0.235248	0.178683	0.110184	0.311705	0.277074
0.15	0.313134	0.304468	0.278979	0.238097	0.184099	0.123983		
0.2	0.314528	0.305962	0.280834	0.240845	0.189203	0.135516	0.314528	0.280836
0.3	0.317212	0.308834	0.284382	0.246039	0.198488	0.153786	0.317212	0.284383
0.4	0.319756	0.311550	0.287712	0.250822	0.206593	0.167683	0.319756	0.287712
0.5	0.322160	0.314110	0.290822	0.255194	0.213602	0.178564	0.322159	0.290822
0.6	0.324422	0.316512	0.293710	0.259152	0.219598	0.187150	0.324421	0.293710
0.7	0.326542	0.318755	0.296375	0.262702	0.224655	0.193846	0.326542	0.296375
0.8	0.328519	0.320840	0.298817	0.265848	0.228831	0.198836	0.328519	0.298817
0.85	0.329455	0.321822	0.299955	0.267272	0.230602	0.200702		
0.9	0.330354	0.322765	0.301036	0.268597	0.232168	0.202128	0.330354	0.301036
0.95	0.331218	0.323668	0.302062	0.269824	0.233531	0.203080		

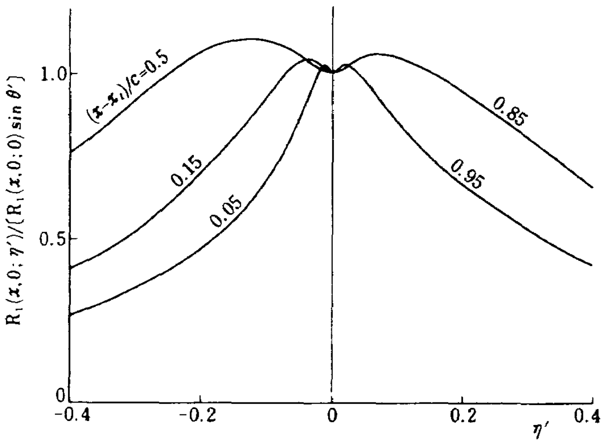

Fig. 1. Variations of Regularized Influence Function for Rectangular Wing of Aspect Ratio 6 with Chordwise Loading Function $\Psi_1(\phi')=\cot(\phi'/2)$

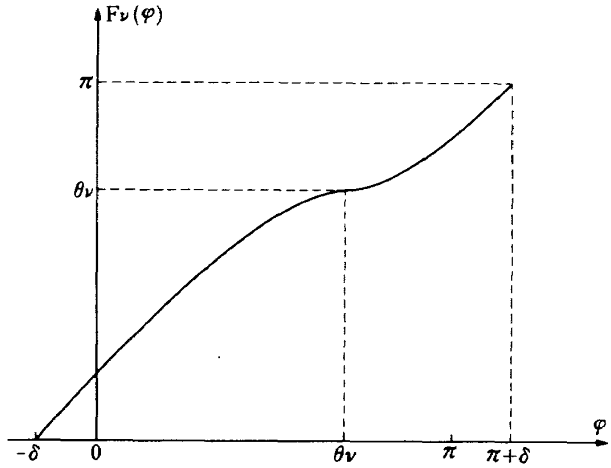

Fig. 2. Function $F_\nu(\varphi)$

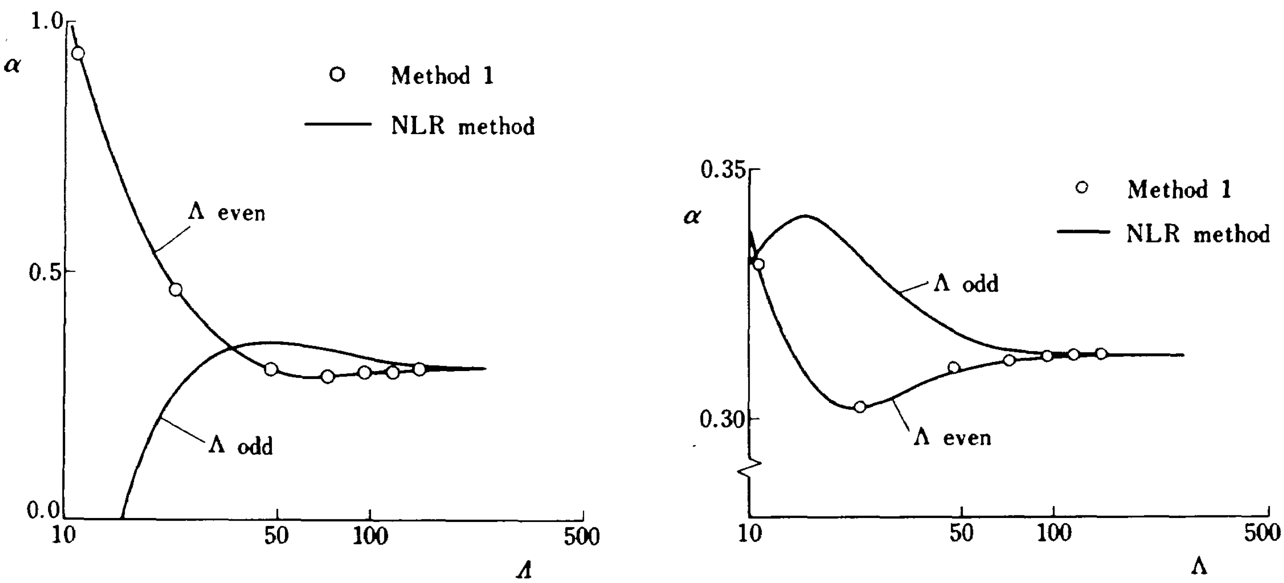

Fig. 3. Comparison of Method 1 with NLR methods for $\eta_\nu=0$

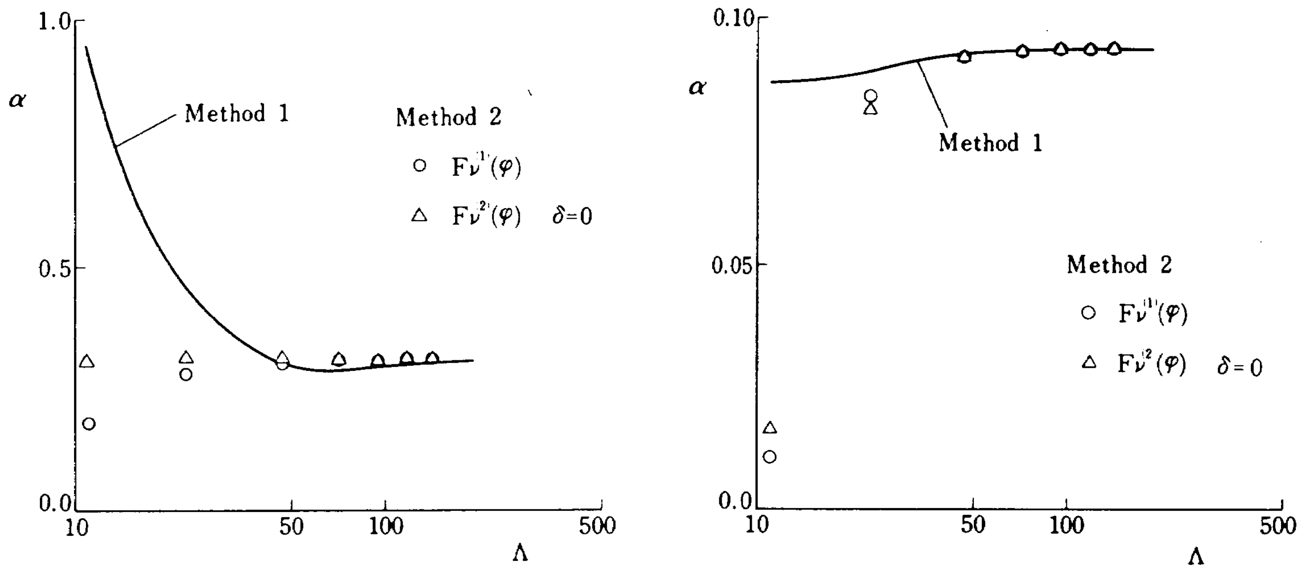

(a) $\eta_\nu=0$ (b) $\eta_\nu=0.965926$

Fig. 4. Comparison of Method 2 ($\delta=0$) with Method 1 for $\xi=0.05$

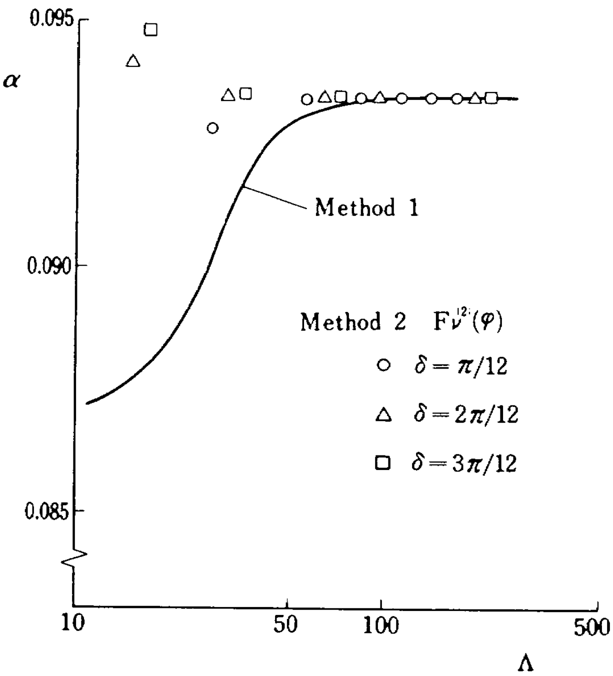

Fig. 5. Comparison of Method 2 ($\delta\neq 0$) with Method 1 for $\xi=0.05$ and $\eta_\nu=0.965926$

TECHNICAL REPORT OF NATIONAL
AEROSPACE LABORATORY
TR-661T

航空宇宙技術研究所報告661T号（欧文）

昭和56年3月発行

発行所　航空宇宙技術研究所
東京都調布市深大寺町1880
電話武蔵野三鷹(0422)47-5911(大代表)〒182

印刷所　株式会社　東京プレス
東京都板橋区桜川2－27－12

Published by
NATIONAL AEROSPACE LABORATORY
1,880 Jindaiji, Chōfu, Tokyo
JAPAN